Oscillations of railway wheelsets with discontinuous model of the contact forces

Máté Antali & Gábor Stépán

antali@mm.bme.hu

Budapest University of Technology and Economics,
Faculty of Mechanical Engineering

Abstract

In this project, the Coulomb friction is used to model the tangential contact forces between the railway wheelset and rails. This results a discontinuous model containing the pure rolling and the pure slipping behaviour. By this approach, a nonsmooth dynamical system is obtained. The condition of transition between rolling and slipping is determined by similar methods to those of piecewise smooth systems

Introduction

We investigate the model of a single railway wheelset running on a straight track with a constant speed v (see Figure 1). We focus on the lateral motion (y) and the yaw rotation (ψ) of the wheelset. In vertical and longitudinal direction, we assume rigid connection between the wheelset and the vehicle, and the resultant effect of lateral and yaw suspensions are modelled by springs.

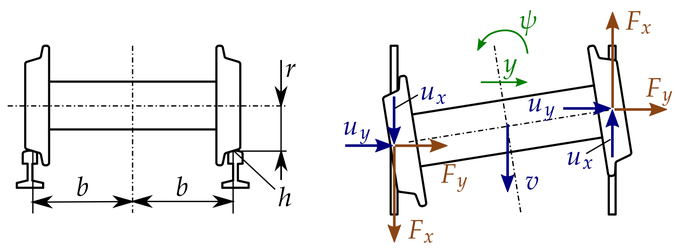

Figure 1: The mechanical model. Left panel: sketch of geometry from front view. The equivalent conicity h depends on also the local geometry of the profiles at the contact points. Right: kinematic variables and friction/creep force components from top view.

Mechanical model

Equations of motion of the wheelset. The two degree-of-freedom model results to the equations of the motion

$$\begin{aligned} J\ddot{\psi} + s_\psi \psi - 2bF_x(u_x, u_y) = 0, \\ m\ddot{y} + s_y y - 2F_y(u_x, u_y) = 0, \end{aligned} \tag{1}$$

which can be found in the literature (see e.g. [1]). The notations can be found in Table 1.

y	lateral displacement	m	mass of the wheelset
ψ	yaw angle	J	moment of inertia
u_x, u_y	creep velocities	s_y	lateral stiffness
v	vehicle speed	s_ψ	yaw stiffness
b	half track width	F_x, F_y	friction/creep forces
r	rolling radius	C	Coulomb friction force
h	equivalent conicity	k_x, k_y	creep coefficients

Table 1: Notations of the mechanical model (1)-(2)-(3).

Approximate values of creep velocities. By using the assumption $h \ll 1$, the linear approximation of the creep velocities become

$$u_x \approx b\dot{\psi} + vh/r \cdot y, \qquad u_y = \dot{y} - v\psi. \tag{2}$$

Nonlinear creep model In the literature, nonlinearity in the creep forces are usually described by a piecewise polynomial model (see e.g. [2]). In this analysis, we consider the nonlinear creep model

$$F_x(u_x, u_y) = -C\frac{u_x}{\sqrt{u_x^2+u_y^2}} \tanh\left(\frac{k_x}{Cv}\sqrt{u_x^2+u_y^2}\right), \tag{3}$$

and the formula for F_y is constructed analogously. In the limit cases, we get:

- Limit case 1 (linear creep model, applied first by [3]):

$$\sqrt{u_x^2+u_y^2} \ll \frac{Cv}{k_x} \qquad \rightarrow \qquad F_x(u_x, u_y) \approx -k_x\frac{u_x}{v} \tag{4}$$

- Limit case 2 (Coulomb friction model):

$$\sqrt{u_x^2+u_y^2} \gg \frac{Cv}{k_x} \qquad \rightarrow \qquad F_x(u_x, u_y) \approx -C\frac{u_x}{\sqrt{u_x^2+u_y^2}} \tag{5}$$

In this analysis, we consider the Coulomb model (5), which is, thus, a consistent limit case of the nonlinear creep model.

Dynamics with the Coulomb model

Slipping dynamics Equations (1), (2) and (5) lead to the following system of 4 first-order ordinary differential equations (the new notations can be found in Table 2):

$$\begin{aligned} \dot{u}_x &= -\left(\alpha_x^2 - \omega^2\right)x + \frac{\omega}{\lambda}u_y - \eta\kappa\frac{u_x}{\sqrt{u_x^2+u_y^2}}, \\ \dot{u}_y &= -\left(\alpha_y^2 - \omega^2\right)y - \lambda\omega u_x - \kappa\frac{u_y}{\sqrt{u_x^2+u_y^2}}, \\ \dot{x} &= u_x - \frac{\omega}{\lambda}y, \\ \dot{y} &= u_y + \lambda\omega x. \end{aligned} \tag{6}$$

The *discontinuity manifold* Σ is the hyperplane determined by $u = \sqrt{u_x^2+u_y^2} = 0$. This is a nonsmooth dynamical system but it is *not* piecewise smooth (see e.g. [4]), because Σ is a *codimension–2 submanifold* of the state space. From approaching Σ from different directions, we get different limits for the accelerations $\dot{u}_x$ and $\dot{u}_y$.

$x = b\psi$	normalised yaw angle
$\omega = v\sqrt{h/(br)}$	angular frequency of kinematic oscillations
$\lambda = \sqrt{r/(hb)}$	geometric factor from conicity
$\alpha_x = \sqrt{s_\psi/J}$	natural angular frequency of yaw motion
$\alpha_y = \sqrt{s_y/m}$	natural angular frequency of lateral motion
$\eta = mb^2/J$	factor from moment of inertia
$\kappa = 2C/m$	normalised Coulomb friction force

Table 2: Definition of the transformed parameters. For physically relevant parameters, $\lambda \approx 2\ldots10$, $\eta \approx 1\ldots10$.

Rolling dynamics In the discontinuity set Σ, the dynamics is determined by the assumption of pure rolling:

$$\dot{u}_x = 0, \qquad \dot{u}_y = 0, \qquad \dot{x} = -\frac{\omega}{\lambda}y, \qquad \dot{y} = \lambda\omega x. \tag{7}$$

Trajectories of (7) are ellipses defined

$$\lambda^2x^2 + y^2 = A^2 \tag{8}$$

where A is the amplitude of the oscillation expressed by the lateral displacement y.

Transition from rolling to slipping

Failure of standard method Usually, dynamic condition of rolling is determined from the Coulomb model by calculating the static friction force. However, the presented model is *statically indetermined* in the case of rolling, thus this method cannot be applied. Instead, we use dynamical methods of codimension-2 discontinuity sets (see also [5]).

Polar coordinates around the discontinuity set Let us switch to polar coordinates by introducing

- the magnitude $u = \sqrt{u_x^2+u_y^2}$ of creep velocity, and
- the direction angle $\phi = \arctan(u_y, u_x)$ of creep velocity.

The dynamics is given by

$$\dot{u} = \dot{u}_x\cos\phi + \dot{u}_y\sin\phi, \qquad u\dot{\phi} = \dot{u}_y\cos\phi - \dot{u}_x\sin\phi. \tag{9}$$

Attracting and repelling directions If a trajectory of (6) reaches the rolling state $u = 0$ from the direction $\phi = \phi_1$ then

$$\lim_{u\to0} u\dot{\phi}(u, \phi_1, x, y) = 0. \tag{10}$$

Let us define the limit $\dot{u}^*$ of the of the contact points, which has a different value depending on the limit direction ϕ_1:

$$\dot{u}^*(\phi_1, x, y) := \lim_{u\to0} \dot{u}(u, \phi_1, x, y). \tag{11}$$

Then, there are two possibilities (see Figure 2):

- If $\dot{u}^*(\phi_1, x, y) < 0$ then the trajectory is pulled towards Σ (attracting direction).
- If $\dot{u}^*(\phi_1, x, y) > 0$ then the trajectory is pushed away from Σ (repelling direction).

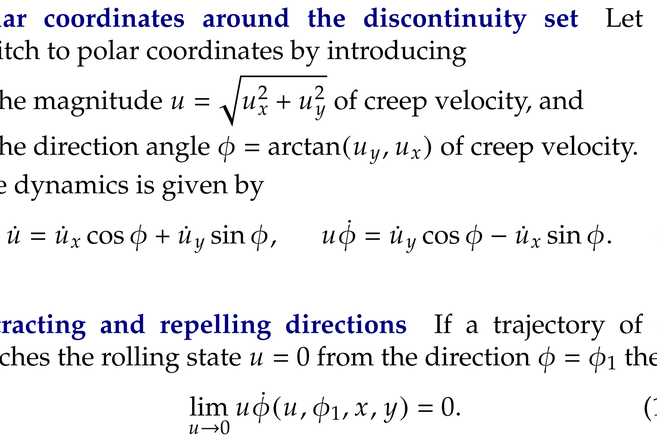

Figure 2: Sketch of the trajectories projected into the orthogonal space of Σ at two example points. The brown lines denote the attracting or repelling directions. Left panel: at this point, we have four attracting directions. In this case, the trajectories cannot escape from Σ, that is, there is no transitions from rolling to slipping. Right panel: ϕ_1 is a repelling direction and ϕ_2 is an attracting direction. Trajectories can escape from Σ along ϕ_1, which means transition from rolling to slipping.

Results

Condition of swithing from rolling to slipping By calculating the criteria prescribed above, we get the the ellipse

$$\left(\alpha_x^2 - \omega^2\right)^2x^2 + \eta^2\left(\alpha_y^2 - \omega^2\right)^2y^2 = \kappa^2\eta^2. \tag{12}$$

Inside the ellipse, there are only attracting directions, and the rolling dynamics (7) is valid (see Figure 3). Outside the ellipse, there is an instantaneous transition to the slipping dynamics (6), the trajectory goes out to the 4 dimensional state space.

By comparing (8) and (12), the maximum admissible amplitude of the oscillation without slipping is $A_{max} = \min(A_1, A_2)$, where

$$A_1 = \frac{\kappa\eta\lambda}{|\alpha_x^2 - \omega^2|}, \qquad A_2 = \frac{\kappa}{|\alpha_y^2 - \omega^2|}. \tag{13}$$

The results can be seen in Figure 4. The intersection $A_1 = A_2$ occurs at

$$\omega_I = \sqrt{\frac{\eta\lambda\alpha_y^2 + \alpha_x^2}{\eta\lambda + 1}}, \qquad \omega_{II} = \sqrt{\frac{\eta\lambda\alpha_y^2 - \alpha_x^2}{\eta\lambda - 1}}. \tag{14}$$

If $\alpha_x^2 > \eta\lambda\alpha_y^2$ then ω_{II} vanishes. At these values, the ellipses (8) and (12) are proportional. Then, at the critical amplitude $A_1 = A_2$, a trajectory of (7) lays exactly on the boundary of the slipping.

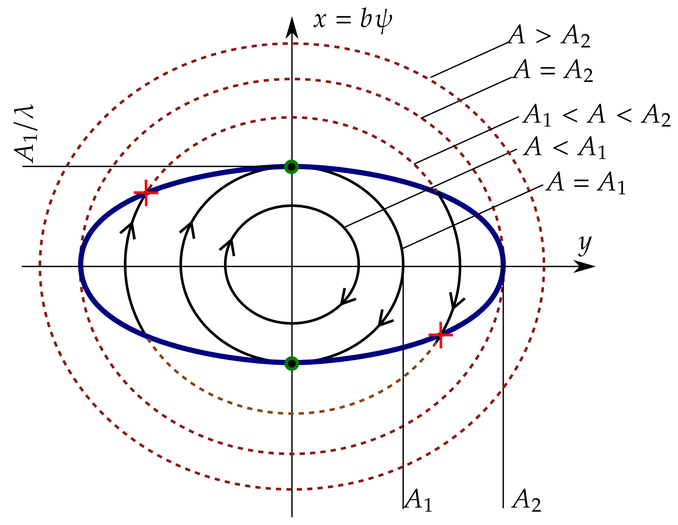

Figure 3: Sketch of the phase portrait of (7). The black solid lines denote the valid rolling trajectories. The blue ellipse denotes the boundary of the slipping. At the red crosses, the trajectories reach the boundary and they escape to the 4 dimensional space described by (6). The brown dotted lines denote virtual trajectories which are not realised due to slipping.

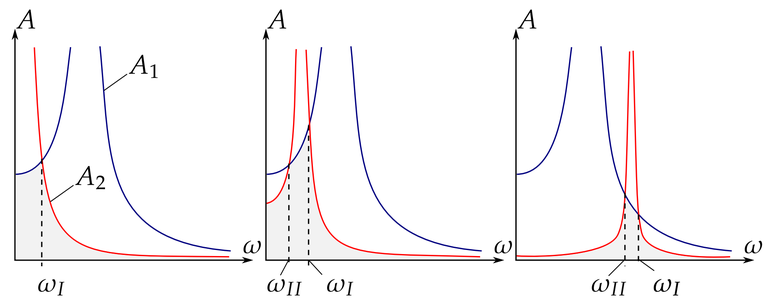

Figure 4: Maximum admissible amplitude of oscillations without slipping. The shaded area denote the region where rolling is possible, and outside that, slipping occurs.The sub-figures denote the three typical cases according to the natural frequencies α_x and α_y. Left: $\alpha_x^2 > \eta\lambda\alpha_y^2$. Middle: $\eta\lambda\alpha_y^2 > \alpha_x^2 > \alpha_y^2$. Right: $\alpha_y^2 > \alpha_x^2$.

Conclusions

From the result, we can propose the following conclusions:

- The Coulomb friction model is a consistent limit case of the nonlinear creep model for large creeps.
- The description by a nonsmooth dynamical system provides a method for calculating the condition of slipping.
- We obtained the maximum admissible amplitude of oscillations without slipping of the wheelset.
- Forthcoming research: Properties of oscillations at the boundary could be possibly used to determine the periodic solutions in the slipping region.

References

[1] J. P. Meijaard: The motion of a railway wheelset on a track or on a roller rig, *Procedia IUTAM 19 274 – 281*, 112:151–157, 2016.

[2] P. J. Vermeulen, K. L. Johnson : Contact of Nonspherical Elastic Bodies Transmitting Tangential Forces, *Journal of Applied Mechanics*, 31(2):338–340, 1964.

[3] F. W. Carter: On the action of a locomotive driving wheel, *Proc. Roy. Soc. A*, 112:151–157, 1926.

[4] M. di Bernardo and et al.: *Piecewise-smooth Dynamical Systems*, Springer, 2008.

[5] M. Antali, G. Stepan: Nonsmooth bifurcations of a dual-point-contact ball, *Nonlinear dynamics*, 83:685–702, 2016.

Acknowledgements

The research leading to these results has received funding from the European Research Council under the European Union's Seventh Framework Programme (FP/2007-2013), ERC Advanced Grant Agreement n. 340889. A.M.D.G.